

# Bag All You Need: Learning a Generalizable Bagging Strategy for Heterogeneous Objects

Arpit Bahety<sup>\*1</sup> Shreeya Jain<sup>\*1</sup> Huy Ha<sup>1</sup> Nathalie Hager<sup>1</sup>  
 Benjamin Burchfiel<sup>2</sup> Eric Cousineau<sup>2</sup> Siyuan Feng<sup>2</sup> Shuran Song<sup>1</sup>  
[bag-all-you-need.cs.columbia.edu](mailto:bag-all-you-need.cs.columbia.edu)

**Abstract**—We introduce a practical robotics solution for the task of heterogeneous bagging, requiring the placement of multiple rigid and deformable objects into a deformable bag. This is a difficult task as it features complex interactions between multiple highly deformable objects under limited observability. To tackle these challenges, we propose a robotic system consisting of two learned policies: a rearrangement policy that learns to place multiple rigid objects and fold deformable objects in order to achieve desirable pre-bagging conditions, and a lifting policy to infer suitable grasp points for bi-manual bag lifting. We evaluate these learned policies on a real-world three-arm robot platform that achieves a 70% heterogeneous bagging success rate with novel objects. To facilitate future research and comparison, we also develop a novel heterogeneous bagging simulation benchmark that will be made publicly available.

## I. INTRODUCTION

Imagine packing a bag for a picnic; we might first put several rigid objects (such as an apple and a water bottle) into the bag, fold deformable objects (such as a picnic mat and a T-shirt) and then place them on top of the bag opening. We must then lift the bag (another deformable object) in a way that these objects fall inside without spilling. Successful completion of this task requires both a comprehensive understanding of the objects’ physical properties and the capability to plan and integrate multiple manipulation skills. For instance, the robot’s actions must take into account:

- **Object geometry:** objects must be placed and oriented to fit into the bag opening.
- **Object material:** large deformable objects, such as blankets, must be folded or crumpled into a compact configuration prior to packing. This requires manipulation strategies that are conditioned on object material (*i.e.* rigid and deformable).
- **Inter-object dynamics:** the ultimate success of this task is determined jointly by object configurations and the robot’s grasp on the bag during lifting. Crucially, when objects are partially inside a bag (for example, a mat on top of the bag opening), different lifting positions will result in different outcomes. Therefore, a successful approach must decide when a desired *pre-bagging condition* is achieved and, if so, determine a good grasp location(s) to lift up the bag. Here, pre-bagging condition refers to when all objects are sufficiently inside the bag opening, and will fall into the bag with a proper lift.

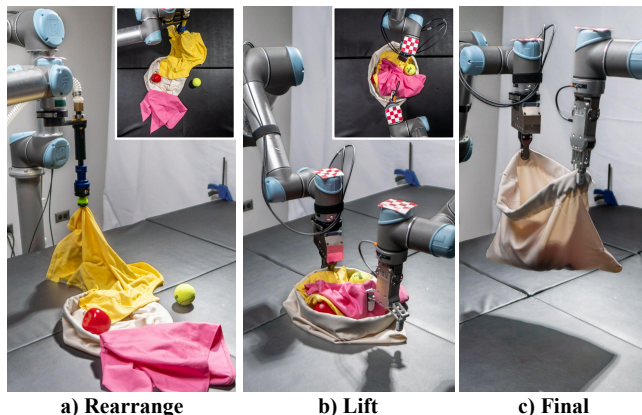


Fig. 1. The **Heterogeneous Bagging Task** requires packing multiple rigid (e.g., the apple) and deformable objects (e.g., the T-shirt) into a deformable bag. The system must learn to (a) strategically manipulate these objects to achieve a feasible pre-bagging configuration. It also needs to (b) infer suitable grasp points from which to lift up the bag such that (c) the objects fall inside the bag.

Due to these difficulties, prior work focused either on only the lifting step of the process [1] or considered a simplified scenario of packing only rigid items [2], [3].

We seek to address these limitations and propose a system that tackles the complete bagging process for a diverse set of rigid and deformable objects — a task we refer to as **heterogeneous bagging**. Our proposed approach consists of two learnable policies: a **rearrangement policy** that uses sequential pick-and-place actions to rearrange or fold items (Fig. 1a) in order to achieve a suitable pre-bagging configuration and a **lifting policy** that determines where to grasp and lift up the bag once pre-bagging conditions are met (Fig. 1b,c). We show that estimating the satisfaction of these pre-bagging conditions (required to decide when to stop rearranging and begin lifting) can be jointly performed by the two policies.

To accomplish this task on real hardware, we develop a representative simulation environment and use it to train both policies. Then, to facilitate a better bridge for the inevitable sim2real gap, we train a *self-supervised* network that detects the bag opening from real-world depth images. These predictions are used as additional input to the rearrangement and lifting policies, allowing them to transfer more robustly from simulation, where they are trained, to the real world.

We evaluate the learned policies with a real-world three-arm robot system with novel objects. The system is equipped with two types of end-effectors: a suction gripper, responsible for

<sup>\*</sup> indicates equal contribution

<sup>1</sup> Columbia University <sup>2</sup> Toyota Research Institute

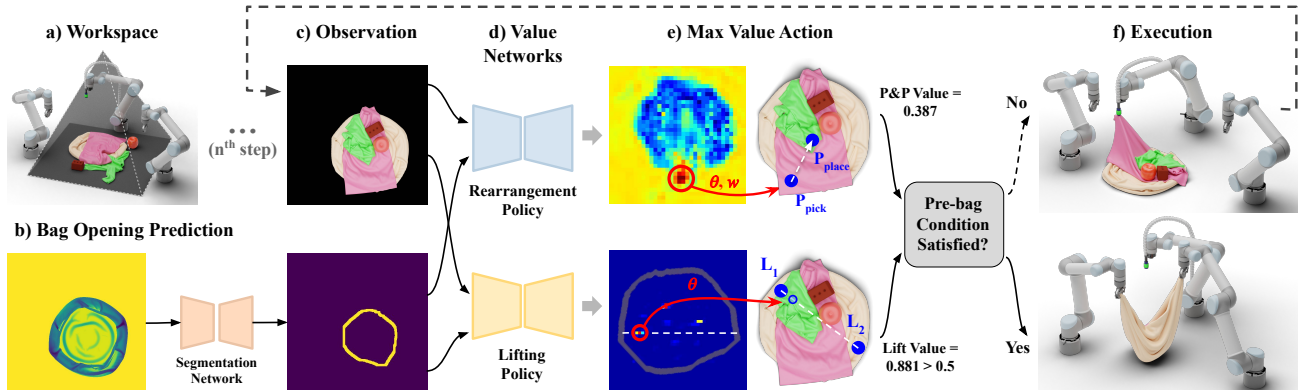


Fig. 2. **Method Overview.** Our system consists of (a) three robot arms and a top camera with a view of the workspace. A top-down depth image of the bag (before placing any other objects) is used to (b) predict the bag opening boundary. For each step, (c) a top-down RGB image and the predicted bag opening mask are input to (d) the rearrangement and lifting policies, which individually output (e) dense value maps and the action corresponding to the highest pick-and-place and lift score. If the pre-bagging condition is satisfied, the bag is (f) lifted from the lift points predicted by the lifting network. Otherwise, we (f) execute a rearrangement action and return to (c) for the next step.

object rearrangement, on one arm and a parallel-jaw gripper, used to perform the bag lifting portion of the task, on the other two arms. We find that our proposed approach achieves a 70% success rate for the heterogeneous bagging task.

The main contribution of this work is the development of the first real-world robot system for the task of heterogeneous bagging. To this end, we propose:

- A self-supervised bag opening detection algorithm from depth images, whose pixel-wise supervision is automatically obtained through color images. This detection result enables robust sim2real transfer for downstream policies.
- A learned rearrangement policy that strategically manipulates and reconfigures multiple rigid and deformable objects to satisfy required pre-bagging conditions.
- A learned lifting policy that determines valid pre-bagging configurations and infers suitable grasp points for a bi-manual bag lifting action.
- A novel simulation environment and benchmark for heterogeneous bagging. The benchmark will be publicly available to facilitate future research and enable a fair comparison between heterogeneous bagging approaches.

## II. RELATED WORK

**Rigid object packing.** Owing to numerous potential real-world applications, the problem of packing rigid objects has been extensively studied [4], [5]. In the offline setting, where the set of items and packing order are predetermined, prior works have primarily focused on exact algorithms [6], heuristics and metaheuristics [7], [8]. In the online setting, where arbitrary items arrive sequentially and must be packed in the order they are received, deep reinforcement learning strategies [2], [3], and the NDOP/QOP algorithm for the nondeterministic order setting [9] have been used. However, all these approaches are limited to packing *rigid*, generally cuboidal, objects into *rigid* containers and are not suitable for deformable objects or non-rigid containers such as bags.

**Cloth and rope manipulation.** Early attempts at deformable object manipulation focused on methods for manipulating one-dimensional deformable objects such as ropes and cables [10]–

[15] and two-dimensional deformable objects such as fabrics [16]–[20]. Data-driven techniques such as Reinforcement Learning and Imitation Learning have also been developed for cloth smoothing [21], [22], folding [23]–[25], and unfolding [26], [27]. While our approach is inspired by some of the prior works in fabric folding, we address a significantly harder task that involves 3D deformable objects such as bags and complex interactions between multiple deformable objects.

**Bag manipulation.** The manipulation of 3D deformable objects, such as bags, is an under-studied research area in robotics due to the inherent complexity and difficulty of the task. Initial work involved calculating the deformation characteristics of an object and determining the minimum lifting force through iterative lifting [28]. Recent relevant studies involve grasping randomly or at maximum width to lift a bag using a physical robot [1] or opening a deformable bag and maintaining the opened state using air-based blowing actions [29].

The most relevant work to our task is perhaps Seita et al. [15], where the task is to insert a rigid object into a deformable bag. But their approach is limited to handling a single rigid object placement and further simplifies the bag lifting task by attaching rigid beads around the bag opening. In contrast, our system can manipulate multiple objects (either rigid or deformable) and infer lift points for a fully-deformable bag directly from real-world RGB-D images, resulting in a more practical solution for real-world applications.

## III. METHOD

### A. Task and System Setup

We formulate the bagging task as follows: First, a bag is placed on a flat surface with its mouth open and facing upward. From this configuration, the robot perceives the bag and infers the bag opening (Fig. 2b). Note that this predicted bag opening remains constant throughout the episode. We then position all the objects randomly across the workspace (Fig. 2a). The robot manipulates and iteratively rearranges these objects to obtain a desirable pre-bagging configuration, estimates a pair of bag-lifting grasp points, and attempts to lift the bag. Finally, a bag-shaking primitive is executed to help

the objects either drop inside the bag or fall out. We define success as no objects touching the surface of the workspace at the end of this sequence (*i.e.* all objects are inside the lifted bag). Refer to Fig. 2 for an overview of the pipeline.

Our simulation environment is built on top of the PyFleX bindings to Nvidia FleX [26], [29]–[31]. In addition to simulating arbitrary cloth meshes and robot end-effectors, our simulator provides the functionality to load arbitrary rigid objects. The simulated training objects include a bag, primitive rigid objects, a subset of the YCB dataset [32], [33]), and rectangular cloths (Fig. 4). The object colors are randomized and observations are rendered using Blender 3D.

Our real-world setup consists of three 6-DoF robot arms, two equipped with parallel-jaw grippers and the third with a suction gripper. To perceive the workspace, the robots obtain a top-down RGB-D image from an Azure Kinect sensor.

### B. Self-supervised Bag Opening Detection

A reliable bag opening detection is critical to the success of our approach. However, due to significant visual differences between the real-world and the simulated bag, an algorithm trained in simulation would face difficulty generalizing to real-world images. Meanwhile, pixel-wise bag opening annotations in the real world are expensive to obtain.

To tackle the above challenges, we propose a self-supervised model where the pixel-wise label is automatically obtained from RGB images of a bag with a colored opening. Concretely, as depicted in Fig. 3, we color the opening of the training bag in the real world blue and use this color information to obtain a segmentation label. We use a filled opening mask (refer to *Label* in Fig. 3) as supervision to avoid the class imbalance issue. We then train a U-Net [34] based segmentation network with Dice Loss [35] to predict the filled mask from depth images. During inference (Fig. 3), the segmentation network takes in a depth image and outputs a mask of the estimated bag opening. The system then post-processes this prediction to obtain only the boundary of the bag opening. The raw predicted mask and the post-processed mask boundary are used as additional inputs to the rearrangement and the lifting policy, respectively.

In simulation, we can use the initial bag configuration to obtain the ground truth opening mask, which is then input to the rearrangement and lifting policies. This shared bag opening representation allows the downstream policies to perform direct sim2real transfer without any real-world finetuning.

### C. Rearrangement Policy

A crucial part of the bagging task is to learn how to rearrange objects such that a good pre-bagging configuration is achieved; the object rearrangement policy is responsible for this. To achieve a valid pre-bagging configuration, the policy must learn how to place objects inside the bag opening while ensuring no object is neglected. Moreover, the policy needs to learn when to stop rearranging to avoid deteriorating a sufficiently good pre-bagging configuration and/or needlessly increasing the number of rearrangement steps.

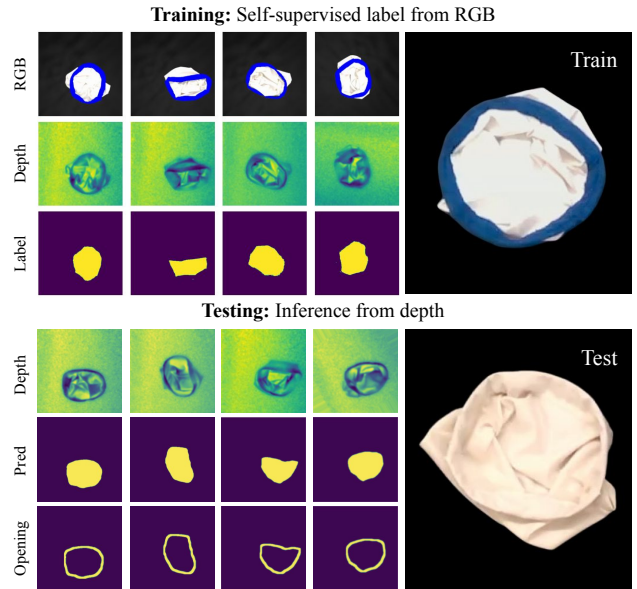


Fig. 3. **Self-supervised Bag Opening Detection.** We color the opening of the training bag in the real world blue and use this color information to automatically obtain a pixel-wise label. The segmentation network is trained to predict this bag opening mask from depth images.

**Action parameterization and network.** The rearrangement policy takes a top-down RGB image and the bag opening mask as input and outputs pick and place pixels,  $P_{\text{pick}}, P_{\text{place}} \in \mathbb{R}^2$ , which can be depth-projected to get 3D locations.

We use the spatial action map policy formulation [26], [36]–[38] and parameterize pick-and-place with  $P_{\text{pick}}$  representing the maximum value pixel from the value network’s output,  $\theta \in \mathbb{R}$  for the planar rotation and  $w \in \mathbb{R}$  for the distance of  $P_{\text{place}}$  from  $P_{\text{pick}}$ . The top-down color image and bag opening mask are concatenated ( $H \times W \times 4$ ) and used to generate a batch of rotated and scaled observations ( $t \times H \times W \times 4$ ). The network takes this batch as input and outputs a corresponding batch of predicted dense value maps ( $t \times H \times W$ ). The  $\text{argmax}$  of the value maps gives us  $P_{\text{pick}}$ , rotation  $\theta$  and scale  $w$  (Fig. 2e), which are then used to compute  $P_{\text{place}}$ . The value of each pixel corresponds to the predicted reduction of volume of all the objects outside the bag opening and thus, we choose the pixel with the maximum value. In our experiments, we use 12 rotations in the range of  $[-180^\circ, 180^\circ]$  and 8 scale factors in the range of  $[1.00, 2.75]$  at 0.25 intervals (giving  $t = 96$ ). The value network is implemented as a U-Net.

**Supervision and training.** The policy is trained via a self-supervised epsilon-greedy exploration in simulation. During a training episode, a random task (refer to Section IV-A) is sampled and each rearrangement step is automatically labeled with the relative change in the volume of all the objects outside the bag opening:  $\Delta v/v = (vol_{\text{pre}} - vol_{\text{post}}) / \max\{vol_{\text{pre}}, vol_{\text{post}}\}$ , where  $vol_{\text{pre}}$  and  $vol_{\text{post}}$  are the pre-action and post-action volumes. A reward of  $-0.5$  is given for pick points on the bag to ensure that  $P_{\text{pick}}$  is not on the bag during inference. Note that this supervision signal (*i.e.* object particles) is neither available nor required during real-world deployment. The robot manipulates objects with the rearrangement policy until no valid grasp is predicted (*i.e.* the highest value action is not on any



object) or reaches the maximum interaction iterations (*i.e.* 10). The network is supervised via MSE loss between predicted and actual  $\Delta v/v$  and is trained using the Adam optimizer [39] with a learning rate of  $1e-3$  and a weight decay of  $1e-6$ . The network is trained to convergence, which takes around 40K simulation steps or about 32 hours on 4 NVIDIA RTX3090s.

#### D. Lifting Policy

The final step of a bagging task is to lift the bag such that all objects fall inside. Accordingly, the lifting policy must predict a pair of points that are likely to be graspable and enable a successful lift. Secondly, it must determine when to take over from the rearrangement policy because a valid pre-bagging configuration has been achieved. Oftentimes, there is a significant nuance to this determination; for instance, a valid pre-bagging configuration may have a T-shirt’s sleeve extend beyond the bag opening but have its center of mass inside.

**Action parameterization and network.** The lifting policy takes a top-down RGB image and the bag opening mask as input and outputs a lifting score with the corresponding lift points,  $L_1, L_2 \in \mathbb{R}^2$ , which can be depth-projected to get 3D locations. To constrain the system to predict lift points on the estimated mouth of the bag, we formulate the action parameterization as  $\langle P_{\text{lift}}, \theta \rangle$ , where  $P_{\text{lift}}$  is a pixel that lies on a line and  $\theta \in \mathbb{R}$  determines the slope of the line. The intersection of the line with the bag opening gives the two lift points,  $L_1, L_2$  (Fig. 2e). To minimize collisions, we ensure that the distance between  $L_1$  and  $L_2$  does not exceed a given physical limit and is greater than the safe distance.

The concatenation of the top-down color image and bag opening mask is used to produce a batch of rotated observations ( $t \times H \times W \times 4$ ). This is input to the network and a corresponding batch of dense value maps ( $t \times H \times W$ ) is predicted. Each pixel in each value map contains the value of the action parameterized by that pixel’s location, providing  $P_{\text{lift}}$ , and the rotation applied to the input observation, providing  $\theta$ . The pixel value corresponds to the predicted probability of lifting success. At runtime, the robot selects the action with the highest predicted value. In our implementation, we use 12 rotations in the range of  $\theta$  to  $[-90^\circ, 90^\circ]$  (giving  $t = 12$ ). The value network is implemented as a U-Net.

**Supervision and training.** The tasks for training the lifting network are generated from our trained rearrangement policy. Each lifting step is labeled as a 1 for success and 0 for failure, where success is defined as no object touching the surface of the workspace after a successful lift. The policy is trained similarly to the rearrangement policy but supervised via a binary cross-entropy loss. The training takes around 100K simulation steps or about 72 hours on 4 NVIDIA RTX3090s

#### E. Verifying Pre-bagging Conditions

The robot uses the output of both policies to determine if the pre-bagging conditions are satisfied. This is beneficial since each policy is trained with different objectives: there are cases when the rearrangement policy predicts an action to further reduce the volume of objects outside the bag opening while the lifting policy predicts that the current configuration

is sufficient for success. In this scenario, it is inefficient and unnecessary to continue rearranging items. At other times, the lifting policy may not be certain that the pre-bagging conditions are met, but the rearrangement policy infers that there is no action that can improve the configuration. In this case, the system should proceed with the lifting action.

At each step, the lifting score is evaluated to achieve this fused pre-bagging determination. If the lifting score is greater than a threshold (0.95 in simulation and 0.5 in real-world), the rearrangement stops and the lift action is executed (Fig. 2). Otherwise, the rearrangement policy predicts an action, and if the action is to terminate, then the bag is lifted from the points corresponding to the highest score predicted previously by the lifting policy.

### IV. EVALUATION

#### A. Experiment Setup

We use three metrics to evaluate system performance: 1) Success rate (**SR**):  $\text{successful\_episode} / \text{total\_episodes}$ , where a successful episode is defined in Section III-A. 2) Average fraction of objects inside the bag (**AvgF**): The number of objects not touching the ground after lifting and shaking the bag divided by the total number of objects in that episode, averaged across all episodes. 3) Average episode length (**AvgL**): The total number of rearrangement steps plus the lifting step in an episode, averaged across all episodes. We evaluate on the following task setups: two (1r1c), three (1r2c, 2r1c), four (1r3c, 2r2c, 3r1c), and five (2r3c, 3r2c) objects, where #r and #c denote the number of rigid objects and cloths.

**Simulation tasks.** During testing, we use a subset of YCB objects (different from training) and CLOTH3D [40] (Fig. 4). Each task has a randomly-sized bag that is kept open on the ground and 2-5 objects arranged in an arbitrary configuration in the workspace. To generate different initial configurations of the bag and randomly-sized cloths (generally larger than the bag opening), they are randomly picked and dropped on the surface. We also ensure that the objects are not entirely inside the bag opening in the initial configuration.

**Real-world tasks.** The testing objects are a subset of YCB, soft toys, T-shirts, pants, and rectangular cloths (Fig. 4). We run 5 different task configurations for the 2 objects case and 10 configurations for each of the 3-5 objects cases.

**Baseline algorithms.** Since there are no existing methods for the task of heterogeneous object bagging, we design strong heuristic baselines for comparison. The heuristic policies in simulation differ from real-world due to the availability of ground truth bag opening.

- **Heuristic rearrangement policy:** In addition to the information that our policy receives, the heuristic policy receives object masks as input. The policy selects a random point on the part of object mask that is non-overlapping with the bag opening mask and places it at the center of the bag opening. Intuitively, this heuristic is reasonable since placing objects at the center would likely reduce the volume of objects outside the bag opening. Instead of a bag opening mask, the real-world heuristic policy uses

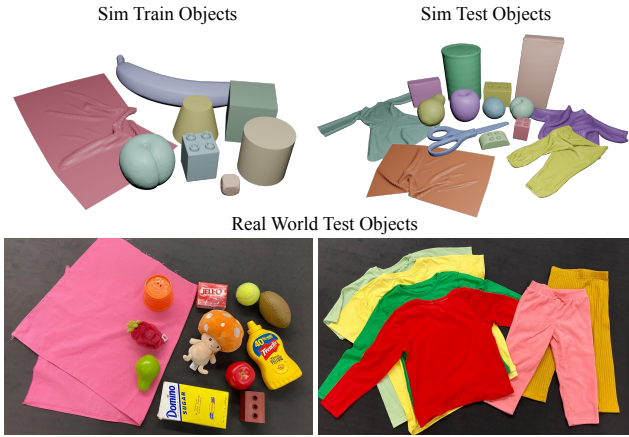


Fig. 4. **Train and Test Objects** used in our experiments. The policy is always tested with novel objects not seen during training.

TABLE I  
SUCCESS RATE IN SIMULATION. L: LEARNED, H: HEURISTIC

Rearrange	Lift	Train Obj	2	3	4	5
H	H	-	75%	50.5%	23.3%	11%
H	L	mixed	89%	73.5%	45.3%	28.5%
L	H	mixed	80%	61%	35.3%	22.5%
L	L	single-rigid	83%	67%	48%	32%
L	L	single-cloth	89%	76%	55%	39%
L	L	mixed	<b>92%</b>	<b>81.5%</b>	<b>75.6%</b>	<b>61.5%</b>

a bag mask computed using color information. The rearrangement is terminated and the bag is lifted when either no pick point is found or the episode length reaches 10.

- **Heuristic lifting policy:** In simulation, the heuristic lifting policy randomly chooses two points on the bag opening mask, with the constraint that the distance between them is greater than a threshold. In real-world experiments, the heuristic lifting policy uses the maximum-width lifting strategy proposed by Seita et al. [1]. Note that this heuristic policy does not determine when to stop rearranging.

## B. Experimental Results

**Benefits of learned rearrangement policy.** Comparing H & L (second row) and L & L (last row) in Table I shows the advantages of a learned rearrangement policy. We observe that as the number of objects increases, our method significantly outperforms the heuristic, signifying the importance of learning multi-object interactions for rearranging objects. Real-world experiments also showcase the effectiveness of the learned rearrangement policy. As can be seen in Table II, our policy performs consistently better than the heuristic. Having a rearrangement policy that learns which objects to rearrange and where to place them helps to achieve a good pre-bagging configuration. We also find that learning when to stop rearranging to avoid unnecessary steps or prevent further actions from deteriorating the pre-bagging configuration helps improve the performance of the system.

**Benefits of learned lifting policy.** Comparing L & H (third row) and L & L (last row) in Table I illustrates the advantages of a learned lifting policy relative to the baseline (40%

improvement). Despite being strong due to the availability of ground truth bag opening, the heuristic performs worse than our learned policy because it is unable to learn the critical relationship between lift points and object configurations. It is also incapable of determining when a desirable pre-bagging configuration is achieved and rearrangement can be halted. Our real-world experiments corroborate the effectiveness of a learned lifting policy as well (Table II).

**Effects of different training scenarios.** In order to understand the impact of training task selection, we conducted experiments with two other training scenarios - a single rigid object in each configuration and a single cloth in each configuration. As depicted in Table I, the mixed training scenario performs the best, aligning with our intuition that training on a single object does not allow the policy to reason about multi-object interaction. Furthermore, the single-rigid policy performs worse than the single-cloth policy as it fails to learn appropriate folding strategies for cloths.

**Real-world experiments.** We directly evaluate our simulation-trained rearrangement and lifting policies with real-world robots. To promote policy transfer from simulation to reality, we perform background substitution that is consistent with the simulation environment. We obtain the bag mask (for heuristic) and predict the bag opening (for ours) before any objects are placed. We also use object masks to remove predicted lift points that overlap with objects. Table II shows the performance, averaged over all test episodes, for each task category. Our policy outperforms the heuristic by as much as 60% on the **SR** metric. Moreover, the significantly higher **AvgF** metric (84% vs 22% in the 5 objects case) indicates that our policy drops fewer objects outside the bag.

Fig. 5 illustrates examples of our system and the heuristic approaches operating in the real world. The first two rows demonstrate how heuristically placing all objects at the center of the bag can lead to failure. While our rearrangement policy learns to arrange each object relative to other objects inside the bag opening, the heuristic method places the apple on top of the soft toy, causing it to fall and roll outside the workspace (step 4, second row). This example also exhibits how our lifting policy learns that a partially protruding cloth can still be a valid pre-bagging configuration (green T-shirt). In the second example (the third and fourth rows), our policy successfully determines which object to rearrange so that a desired pre-bagging configuration is obtained. Despite the presence of three cloth objects partially outside the bag opening, our policy rearranges the pear (step 8, third row). In contrast, the heuristic keeps rearranging the cloth and overlooks the pear even though it is clearly outside the bag opening. The third example shows that even when the heuristic rearrangement policy is able to achieve a good pre-bagging configuration, learning from where to lift the bag is crucial. Our policy is able to infer the bag opening and predict optimal lift points, which lead to success, whereas the lift locations chosen by the heuristic lead to failure.

**Failure modes and limitations.** The most common failure case was during bag grasping (accounting for 50% of real-world failures). For instance, the robot would inadvertently



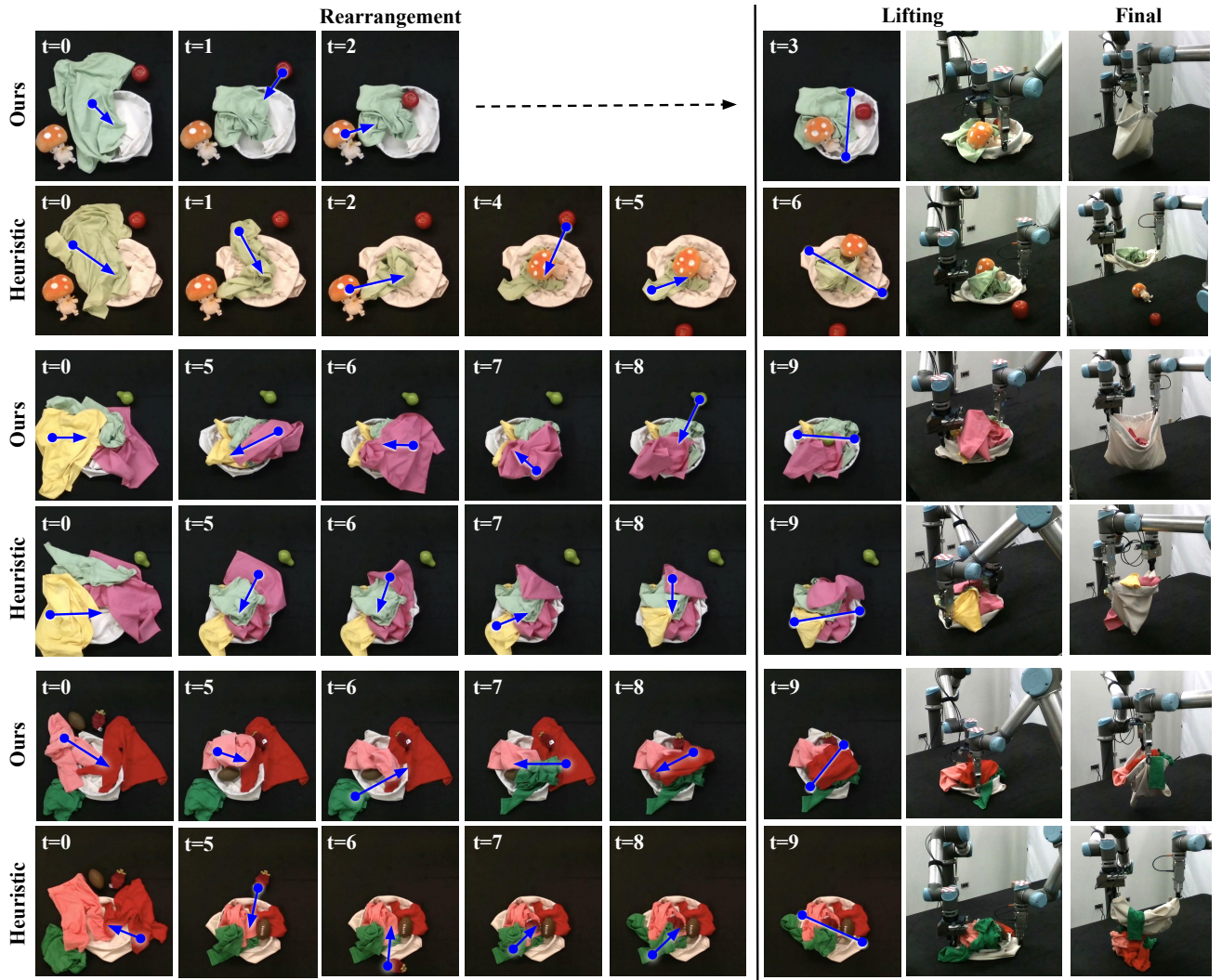


Fig. 5. **Real-world Bagging Results.** The first two examples illustrate how our policy is successfully able to rearrange all objects whereas the heuristic policy fails (the apple rolls away in the first example and in the second, the heuristic repeatedly rearranges the cloths and never the pear). In the third example, even with a good pre-bagging configuration, a heuristic lift fails as it does not find good lift points. More robot videos can be found on the [project website](#).

TABLE II  
REAL-WORLD RESULTS

	Metric	2	3	4	5
Heuristic	SR $\uparrow$	60%	20%	20%	0%
	AvgF $\uparrow$	80.0%	43.3%	37.5%	22.0%
	AvgL $\downarrow$	3.8	5.6	5.9	8.5
Ours	SR $\uparrow$	80.0%	80.0%	70.0%	50.0%
	AvgF $\uparrow$	90.0%	93.3%	87.5%	84.0%
	AvgL $\downarrow$	3.6	4.5	5.7	8.2

grasp a cloth close to one of the predicted lift points and lift the cloth instead of the bag. Closing the loop between the rearrangement and the lifting policy to incentivize rearranging objects away from potential lift points might help resolve this issue. Another observed failure mode is suboptimal object rearrangement (accounting for 32% of real-world failures). For instance, a rigid object placed upon a pile of cloth is generally unstable. This failure is caused by the single-step training reward, causing the rearrangement policy to not explicitly consider object stability for future interactions.

Our method also makes certain assumptions that could be

relaxed in future works: It assumes that the bag is open and flat on a surface, potentially requiring an additional system [29] to achieve this initial configuration. It is also limited to 2D pick and place; future work could consider a more expressive 6-DoF action space capable of inserting objects from the side into a partially open bag held up with one arm.

## V. CONCLUSION

We propose and evaluate a real-world robotic system for the task of heterogeneous bagging which involves placing a diverse set of multiple rigid and deformable objects into a deformable bag. The system includes a self-supervised segmentation network trained to infer the bag opening, a rearrangement policy, and a lifting policy. We demonstrate the effectiveness of our method by comparing it against strong baselines on a set of real-world tasks. We hope that this work encourages others in the field to explore the challenging task of heterogeneous bagging and believe that the lessons learned in this setting have strong potential to transfer to other dexterous manipulation tasks involving the interaction of multiple highly deformable objects.

**Acknowledgements.** This work was supported in part by the Toyota Research Institute, NSF Award #2143601, #2037101, and #2132519. We would like to thank Google for the UR5 robot hardware. The views and conclusions contained herein are those of the authors and should not be interpreted as necessarily representing the official policies, either expressed or implied, of the sponsors.

## REFERENCES

- [1] D. Seita, J. Kerr, J. Canny, and K. Goldberg, “Initial results on grasping and lifting physical deformable bags with a bimanual robot,” in *IROS Workshop on Robotic Manipulation of Deformable Objects in Real-world Applications*, vol. 2, 2021, p. 3.
- [2] H. Zhao, Q. She, C. Zhu, Y. Yang, and K. Xu, “Online 3d bin packing with constrained deep reinforcement learning,” in *Proceedings of the AAAI Conference on Artificial Intelligence*, vol. 35, no. 1, 2021, pp. 741–749.
- [3] H. Zhao, C. Zhu, X. Xu, H. Huang, and K. Xu, “Learning practically feasible policies for online 3d bin packing,” *Science China Information Sciences*, vol. 65, no. 1, pp. 1–17, 2022.
- [4] K. Zakka, A. Zeng, J. Lee, and S. Song, “Form2fit: Learning shape priors for generalizable assembly from disassembly,” in *2020 IEEE International Conference on Robotics and Automation (ICRA)*. IEEE, 2020, pp. 9404–9410.
- [5] A. Zeng, P. Florence, J. Tompson, S. Welker, J. Chien, M. Attarian, T. Armstrong, I. Krasin, D. Duong, V. Sindhwani *et al.*, “Transporter networks: Rearranging the visual world for robotic manipulation,” *arXiv preprint arXiv:2010.14406*, 2020.
- [6] S. Martello and D. Vigo, “Exact solution of the two-dimensional finite bin packing problem,” *Management science*, vol. 44, no. 3, pp. 388–399, 1998.
- [7] B. S. Baker, E. G. Coffman, Jr, and R. L. Rivest, “Orthogonal packings in two dimensions,” *SIAM Journal on computing*, vol. 9, no. 4, pp. 846–855, 1980.
- [8] D. S. Johnson, A. Demers, J. D. Ullman, M. R. Garey, and R. L. Graham, “Worst-case performance bounds for simple one-dimensional packing algorithms,” *SIAM Journal on computing*, vol. 3, no. 4, pp. 299–325, 1974.
- [9] F. Wang and K. Hauser, “Robot packing with known items and nondeterministic arrival order,” *IEEE Transactions on Automation Science and Engineering*, vol. 18, no. 4, pp. 1901–1915, 2020.
- [10] J. E. Hopcroft, J. K. Kearney, and D. B. Kraftt, “A case study of flexible object manipulation,” *The International Journal of Robotics Research*, vol. 10, no. 1, pp. 41–50, 1991.
- [11] M. Saha and P. Ito, “Manipulation planning for deformable linear objects,” *IEEE Transactions on Robotics*, vol. 23, no. 6, pp. 1141–1150, 2007.
- [12] K. Suzuki, M. Kanamura, Y. Suga, H. Mori, and T. Ogata, “In-air knotting of rope using dual-arm robot based on deep learning,” in *2021 IEEE/RSJ International Conference on Intelligent Robots and Systems (IROS)*. IEEE, 2021, pp. 6724–6731.
- [13] C. Chi, B. Burchfiel, E. Cousineau, S. Feng, and S. Song, “Iterative residual policy for goal-conditioned dynamic manipulation of deformable objects,” in *Proceedings of Robotics: Science and Systems (RSS)*, 2022.
- [14] A. Nair, D. Chen, P. Agrawal, P. Isola, P. Abbeel, J. Malik, and S. Levine, “Combining self-supervised learning and imitation for vision-based rope manipulation,” in *2017 IEEE international conference on robotics and automation (ICRA)*. IEEE, 2017, pp. 2146–2153.
- [15] D. Seita, P. Florence, J. Tompson, E. Coumans, V. Sindhwani, K. Goldberg, and A. Zeng, “Learning to rearrange deformable cables, fabrics, and bags with goal-conditioned transporter networks,” in *2021 IEEE International Conference on Robotics and Automation (ICRA)*. IEEE, 2021, pp. 4568–4575.
- [16] J. Sanchez, J.-A. Corrales, B.-C. Bouzgarrou, and Y. Mezouar, “Robotic manipulation and sensing of deformable objects in domestic and industrial applications: a survey,” *The International Journal of Robotics Research*, vol. 37, no. 7, pp. 688–716, 2018.
- [17] C. Bersch, B. Pitzer, and S. Kammel, “Bimanual robotic cloth manipulation for laundry folding,” in *2011 IEEE/RSJ International Conference on Intelligent Robots and Systems*. IEEE, 2011, pp. 1413–1419.
- [18] J. Maitin-Shepard, M. Cusumano-Towner, J. Lei, and P. Abbeel, “Cloth grasp point detection based on multiple-view geometric cues with application to robotic towel folding,” in *2010 IEEE International Conference on Robotics and Automation*. IEEE, 2010, pp. 2308–2315.
- [19] F. Osawa, H. Seki, and Y. Kamiya, “Unfolding of massive laundry and classification types by dual manipulator,” *Journal of Advanced Computational Intelligence and Intelligent Informatics*, vol. 11, no. 5, pp. 457–463, 2007.
- [20] M. Cusumano-Towner, A. Singh, S. Miller, J. F. O’Brien, and P. Abbeel, “Bringing clothing into desired configurations with limited perception,” in *2011 IEEE international conference on robotics and automation*. IEEE, 2011, pp. 3893–3900.
- [21] A. Ganapathi, P. Sundaresan, B. Thananjeyan, A. Balakrishna, D. Seita, J. Grannen, M. Hwang, R. Hoque, J. E. Gonzalez, N. Jamali *et al.*, “Learning dense visual correspondences in simulation to smooth and fold real fabrics,” in *2021 IEEE International Conference on Robotics and Automation (ICRA)*. IEEE, 2021, pp. 11 515–11 522.
- [22] X. Lin, Y. Wang, Z. Huang, and D. Held, “Learning visible connectivity dynamics for cloth smoothing,” in *Conference on Robot Learning*. PMLR, 2022, pp. 256–266.
- [23] F. Ebert, C. Finn, S. Dasari, A. Xie, A. Lee, and S. Levine, “Visual foresight: Model-based deep reinforcement learning for vision-based robotic control,” *arXiv preprint arXiv:1812.00568*, 2018.
- [24] J. Matas, S. James, and A. J. Davison, “Sim-to-real reinforcement learning for deformable object manipulation,” in *Conference on Robot Learning*. PMLR, 2018, pp. 734–743.
- [25] R. Jangir, G. Alenya, and C. Torras, “Dynamic cloth manipulation with deep reinforcement learning,” in *2020 IEEE International Conference on Robotics and Automation (ICRA)*. IEEE, 2020, pp. 4630–4636.
- [26] H. Ha and S. Song, “Flingbot: The unreasonable effectiveness of dynamic manipulation for cloth unfolding,” in *Conference on Robot Learning*. PMLR, 2022, pp. 24–33.
- [27] D. Seita, A. Ganapathi, R. Hoque, M. Hwang, E. Cen, A. K. Tanwani, A. Balakrishna, B. Thananjeyan, J. Ichnowski, N. Jamali *et al.*, “Deep imitation learning of sequential fabric smoothing from an algorithmic supervisor,” in *2020 IEEE/RSJ International Conference on Intelligent Robots and Systems (IROS)*. IEEE, 2020, pp. 9651–9658.
- [28] A. M. Howard and G. A. Bekey, “Intelligent learning for deformable object manipulation,” *Autonomous Robots*, vol. 9, no. 1, pp. 51–58, 2000.
- [29] Z. Xu, C. Chi, B. Burchfiel, E. Cousineau, S. Feng, and S. Song, “Dextairity: Deformable manipulation can be a breeze,” *arXiv preprint arXiv:2203.01197*, 2022.
- [30] X. Lin, Y. Wang, J. Olkin, and D. Held, “Softgym: Benchmarking deep reinforcement learning for deformable object manipulation,” *CoRR*, vol. abs/2011.07215, 2020. [Online]. Available: <https://arxiv.org/abs/2011.07215>
- [31] Y. Li, J. Wu, R. Tedrake, J. B. Tenenbaum, and A. Torralba, “Learning particle dynamics for manipulating rigid bodies, deformable objects, and fluids,” in *International Conference on Learning Representations*, 2019. [Online]. Available: <https://openreview.net/forum?id=rJgbSn09Ym>
- [32] B. Calli, A. Walsman, A. Singh, S. Srinivasa, P. Abbeel, and A. M. Dollar, “Benchmarking in manipulation research: Using the yale-cmu-berkeley object and model set,” *IEEE Robotics & Automation Magazine*, vol. 22, no. 3, pp. 36–52, 2015.
- [33] B. Calli, A. Singh, J. Bruce, A. Walsman, K. Konolige, S. Srinivasa, P. Abbeel, and A. M. Dollar, “Yale-cmu-berkeley dataset for robotic manipulation research,” *The International Journal of Robotics Research*, vol. 36, no. 3, pp. 261–268, 2017.
- [34] O. Ronneberger, P. Fischer, and T. Brox, “U-net: Convolutional networks for biomedical image segmentation,” *CoRR*, vol. abs/1505.04597, 2015. [Online]. Available: <http://arxiv.org/abs/1505.04597>
- [35] C. H. Sudre, W. Li, T. K. M. Vercauteren, S. Ourselin, and M. J. Cardoso, “Generalised dice overlap as a deep learning loss function for highly unbalanced segmentations,” *Deep learning in medical image analysis and multimodal learning for clinical decision support : Third International Workshop, DLMIA 2017, and 7th International Workshop, ML-CDS 2017, held in conjunction with MICCAI 2017 Quebec City, QC, ...*, vol. 2017, pp. 240–248, 2017.
- [36] J. Wu, X. Sun, A. Zeng, S. Song, J. Lee, S. Rusinkiewicz, and T. Funkhouser, “Spatial action maps for mobile manipulation,” *arXiv preprint arXiv:2004.09141*, 2020.
- [37] A. Zeng, S. Song, J. Lee, A. Rodriguez, and T. Funkhouser, “Tossingbot: Learning to throw arbitrary objects with residual physics,” *IEEE Transactions on Robotics*, vol. 36, no. 4, pp. 1307–1319, 2020.

- [38] A. Zeng, S. Song, S. Welker, J. Lee, A. Rodriguez, and T. Funkhouser, "Learning synergies between pushing and grasping with self-supervised deep reinforcement learning," in *2018 IEEE/RSJ International Conference on Intelligent Robots and Systems (IROS)*. IEEE, 2018, pp. 4238–4245.
- [39] D. P. Kingma and J. Ba, "Adam: A method for stochastic optimization," in *3rd International Conference on Learning Representations, ICLR 2015, San Diego, CA, USA, May 7-9, 2015, Conference Track Proceedings*, Y. Bengio and Y. LeCun, Eds., 2015. [Online]. Available: <http://arxiv.org/abs/1412.6980>
- [40] H. Bertiche, M. Madadi, and S. Escalera, "Cloth3d: Clothed 3d humans," in *European Conference on Computer Vision*. Springer, 2020, pp. 344–359.